Distribution of Distances between Different (End or Inner) Units in Θ and Excluded-Volume Polymer Chains

Ana M. Rubio and Juan J. Freire*

Departamento de Química Física, Facultad de Ciencias Químicas, Universidad Complutense, 28040 Madrid, Spain

Marvin Bishop

Department of Mathematics and Computer Science, Manhattan College, Riverdale, New York 10471

Julian H. R. Clarke

Department of Chemistry, University of Manchester Institute of Science and Technology, Manchester M60 QD, U.K.

Received January 5, 1993; Revised Manuscript Received April 20, 1993

ABSTRACT: The distribution of distances between any pair of units in a flexible linear polymer is investigated by an off-lattice Monte Carlo method. Three different cases, according to the position of the pair components (end or inner units), are studied. The results depend upon the Lennard-Jones energy parameter, which determines the solvent regime. For the excluded-volume conditions, the results are in agreement with renormalization group predictions. The results in the Θ region show more subtle features, but they are close to the Gaussian ideal behavior. The equilibrium cyclization probability is also computed.

Introduction

Many important conformational properties of a flexible polymer chain can be characterized from the end-to-end distance distribution function, $F(R)$. In the absence of long-range intramolecular interactions, this function adopts a Gaussian form. If the model chain is composed of units that represent Gaussian subchains whose mean length is considerably larger than the polymer persistence length, a similar form also applies for the distribution of distances between any pair of units i and j. Therefore, in three dimensions, we can consider the general form[1]

$$F(R_{ij}) = (3/2\pi\langle R_{ij}^2\rangle)^{3/2} \exp(-3R_{ij}^2/2\langle R_{ij}^2\rangle) \quad (1)$$

where $\langle R_{ij}^2\rangle$ is the quadratic mean distance between the units. However, $F(R_{ij})$ changes dramatically when one considers a chain with intramolecular interactions between nonneighboring units. Assuming a purely repulsive potential (which describes quite well the realistic case of an isolated polymer chain immersed in a good solvent, i.e., in excluded-volume conditions[2,3]), the Lagrangian theoretical approach followed by des Cloizeaux[4] arrives at a general scaling form in terms of universal exponents

$$t = 1/(1-\nu) \quad (2)$$

(where ν is the scaling exponent of the mean-square end-to-end distance) and θ_k (which is related to the critical exponents[3] ν and γ, where γ is related to the number of conformations). Both exponents are dependent upon the space dimension, d. This dependency varies according to the different possible positions of units i and j along the chain. The renormalization group second-order expansion in $\epsilon = 4-d$ leads to the following results:[4]

Case A: i and j are both end units

$$\theta_0 = \epsilon/4+9\epsilon^2/128 \quad (3a)$$

Case B: i is an end and b is an inner unit close to the center (or vice versa)

$$\theta_1 = \epsilon/2-3\epsilon^2/64 \quad (3b)$$

Case C: i and j are inner units

$$\theta_2 = \epsilon-15\epsilon^2/32 \quad (3c)$$

Another approach by Oono and Ohta[5] gave the same results to first order in ϵ. For $d = 3$, an exact expression for θ_0 exists,[4] $\theta_0 = (\gamma-1)/\nu$. Also, better estimates of θ_1 and θ_2 can be obtained from the Borel integral corresponding to Padé approximant representations based on the form of eqs 3b and 3c. All these theoretical predictions are contained in Table I.

According to Redner,[6] the small and large distance behaviors of $F(R_{ij})$ can be represented by a single general function which, properly normalized, can be written as[7]

$$F(R_{ij}) = C\langle R_{ij}^2\rangle^{-d/2}(R_{ij}^2/\langle R_{ij}^2\rangle)^{\theta_k/2} \exp[-(KR_{ij}^2/\langle R_{ij}^2\rangle)^{t/2}] \quad (4)$$

where

$$K = \{\Gamma[(d+2+\theta_k)/t]/\Gamma[(d+\theta_k)/t]\}^{1/2} \quad (5)$$

(Γ is the Gamma function) and

$$C = tK^{(\theta_k+d)}/\{(\textstyle\int_\Omega d\Omega)\Gamma[(d+\theta_k)/t]\} \quad (6)$$

where $d\Omega$ represents the angular part of $d\mathbf{r}_{ij}$ ($\int_\Omega d\Omega = 4\pi$ for $d = 3$).

Baumgärtner[8] investigated freely joined chains with a hard-sphere potential in three dimensions by means of a Monte Carlo simulation technique. The results confirmed the small R scaling behavior for the end-to-end distance, but numerical fittings of the exponents θ_1 and θ_2 to his results (included in Table I) were not in agreement with the theoretical predictions for θ_1 and θ_2 (eqs 3b and 3c).

Recently, we have shown that eq 4 satisfactorily describes the behavior of the end-to-end distance in the excluded-volume regime, as determined from Monte Carlo and Brownian dynamics[7] simulations of chains in three dimensions with Gaussianly distributed beads and long-range intramolecular interactions.

In this work, we use the same model to perform a Monte Carlo simulation study of the distribution of distances for cases A–C described above. For the calculations involving

0024-9297/93/2226-4018$04.00/0 © 1993 American Chemical Society

Table I[a]

	theoretical[b]	previous Monte Carlo[c]	exact enumeration
θ_0	0.273 ± 0.004	0.270 ● 0.006	0.194[d]
θ_1	0.459 ± 0.003	0.55 ● 0.06	0.61 ± 0.17,[e] 0.70 ± 0.12[f]
θ_2	0.71 ± 0.05	0.9 ● 0.1	0.67 ● 0.34[g]

[a] Values of the exponents θ_k from theory and previous simulations. [b] Reference 4. [c] Reference 8. [d] Reference 14. [e] Reference 15. [f] Reference 16. [g] Reference 6.

inner units we consider $|i\text{-}j| \leq N/2$, where N is the number of units in the chain. In case C, i and j are symmetrically located about the central unit. We use a long-range potential with attractive and repulsive parts that can describe both the excluded-volume and the Θ conditions. The latter situation corresponds to the compensation of both types of interactions which cancels binary interactions and yields a quasi-ideal behavior for many chain properties. Our aim was to make a detailed analysis of the results and to compare them with the theoretical predictions for $F(R_{ij})$, i.e., with eqs 1 and 4, in the different cases. For the excluded-volume conditions, we examined the validity of the theoretical values of the exponents θ_1 and θ_2. For the Θ regime, we discuss the statistical behavior in the different parts of the chain under conditions of global quasi-ideal behavior. The rate constants for a cyclization or ring formation within the chain, involving different pairs of units, have also been obtained.

Methods

Our chain model has been previously described in earlier work.[7,9,10] We consider N Gaussian beads of mean length b (b is adopted as the length unit through the calculations). Nonneighboring beads interact by means of the Lennard-Jones potential

$$U(R_{ij})/k_BT = 4(\epsilon/k_BT)[(\sigma/R_{ij})^{12}\text{-}(\sigma/R_{ij})^6] \qquad (7)$$

The relative energy in the well, ϵ/k_BT, is set so as to reproduce the different regimes. Thus, with the value $\sigma/b = 0.8$ (fixed for all calculations), and $\epsilon/k_BT = 0.1$, we have previously obtained results consistent[7,10] with the predicted scaling laws for excluded-volume chains[2,3] and also with other simulations performed with both lattice[11] and off-lattice[12] hard-sphere models. The choice $\epsilon/k_BT = 0.3$ reproduces the linear dependence of the mean quadratic radius of gyration with chain length, a result characteristic of the quasi-ideal Θ conditions[9] (for values of N smaller than 100). A value of $\epsilon/k_BT = 0.275$ seems to be the appropriate Θ regime choice for longer chains.[10]

We have employed a Monte Carlo algorithm also described in previous work.[9] It starts by building an initial chain conformation of moderate energy. New conformations are then generated by selecting a bead and resampling each of its components with respect to the preceding unit along the chain from the appropriate Gaussian distribution. The rest of the chain, up to its closest end, is rotated and then connected with this new bead. A Metropolis energy criterion is used for the acceptance or rejection of conformations. This sampling method (a form of the pivot algorithm) is efficient for excluded-volume conditions. However, in order to probe the Θ region, we use a different method in which, once the chosen bead is placed in its new position, the rest of the chain is not rotated but simply translated.

Eight runs are performed, each one starting with a different seed number and each attempting 50 000 conformations (150 000 × 8 conformations for the longest chains). Finally, the properties are averaged over all the conformations and independent runs. The distribution of distances is obtained by computing the histogram corresponding to a grid of values of R. $F(R)$ is evaluated from this histogram through a normalization which takes into account the total number of conformations and the volume associated with the different grid intervals. We have also calculated mean-squared distances $\langle R_{ij}^2 \rangle$ and the cyclization probabilities $F(R_{ij}=0)$, which are directly related to ring formation rate constants.[13] These were evaluated by counting the number of conformations for which the distance between units i and j is smaller than a given value R_0 (set equal to $2b$). A normalization which includes the allowed cyclization spherical volume is also performed.

Table II[a]

	$\langle R_{ij}^2 \rangle / b^2$ for $\epsilon/k_BT = 0.1$		
$\|i\text{-}j\|$	A	B	C
12	18.70	19.57	21.67
24	42.18	44.94	48.07
36	68.40	72.63	77.77
48	96.85	101.27	108.72
60	124.79	131.62	138.98
72	154.41	162.56	179.96
ν^*	0.594 ± 0.002	0.591 ± 0.002	0.586 ± 0.005

[a] $\langle R_{ij}^2 \rangle / b^2$ for the excluded-volume conditions and the three different cases explained in the text. In cases B and C involving inner units, the chain is $N = 145$. The asterisk indicates that this value is from a ln–ln linear fit, using eq 8.

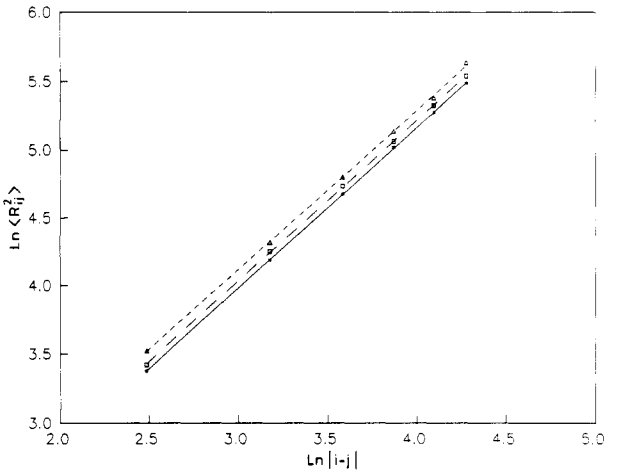

Figure 1. ln–ln plots of $\langle R_{ij} \rangle$ vs $|i\text{-}j|$ for $N = 145$ and cases A (△), B (□) and C (*).

Results and Discussion

(a) Excluded Volume. Table II shows results for $\langle R_{ij}^2 \rangle$ corresponding to the three different cases according to the location of units i and j (cases A–C defined in the Introduction) and the choice of ϵ/k_BT corresponding to the excluded-volume conditions. Fits to the scaling law[3]

$$\langle R_{ij}^2 \rangle \sim |i\text{-}j|^{2\nu} \qquad (8)$$

as shown in Figure 1, lead to the values of ν also included in Table II. For $\epsilon/k_BT = 0.1$, these numerical values are very close to the theoretical prediction for the critical exponent ν in three dimensions,[2,3] $\nu = 0.588$. Accordingly, our simulations with this particular choice of ϵ/k_BT can be assumed to correspond to the excluded-volume regime.

We have compared our data with the des Cloizeaux function, i.e., eq 4 with the values of θ_k indicated in the

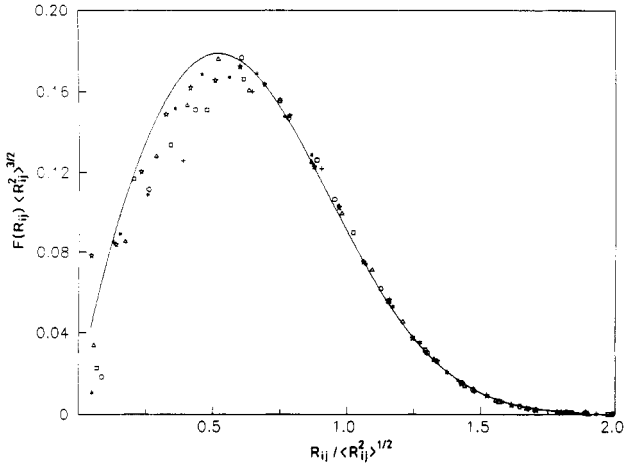

Figure 2. Scaled end-to-end distance distribution function $F(R_{ij})\langle R_{ij}^2\rangle^{3/2}$ vs $R_{ij}/\langle R_{ij}^2\rangle^{1/2}$ for EV chains in case C with N = 145 and different $|i\text{-}j|$ values: (+) 12, (○) 24, (□) 36, (△) 48, (*) 60, (☆) 72. Solid line: results from the des Cloizeaux function (eq 4).

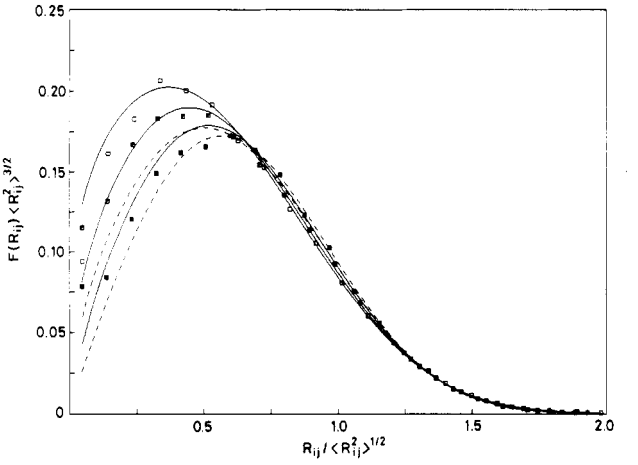

Figure 3. Scaled end-to-end distance distribution function $F(R_{ij})\langle R_{ij}^2\rangle^{3/2}$ vs $R_{ij}/\langle R^2\rangle^{1/2}$ in cases A–C for EV chains with $|i\text{-}j|$ = 72 (N = 145 for cases B and C). The curves are obtained from eq 4 with θ_k according to eqs 3a and 3b (—) and according to Baumgärtner[8] (- - -).

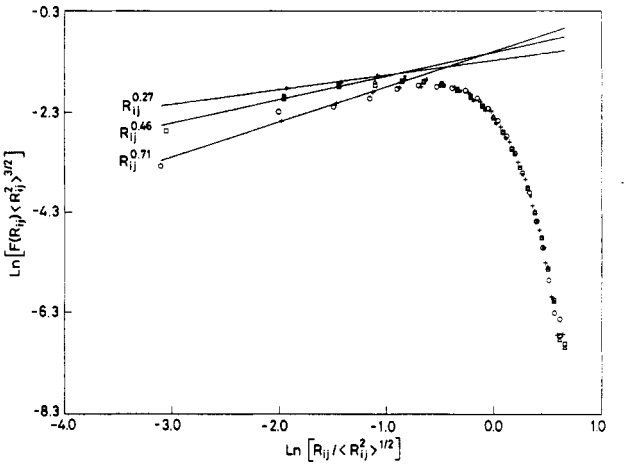

Figure 4. ln–ln plot of $F(R_{ij})\langle R_{ij}^2\rangle^{3/2}$ vs $R_{ij}/\langle R^2\rangle^{1/2}$ for the same chains of Figure 3: (*) case A, (△) case B, (+) case C, (—) small R_{ij} regime for the des Cloizeaux function with the theoretical values of θ_k exponents as indicated in the second column of Table I. Results for a chain with N = 313: (□) case B, (○) case C.

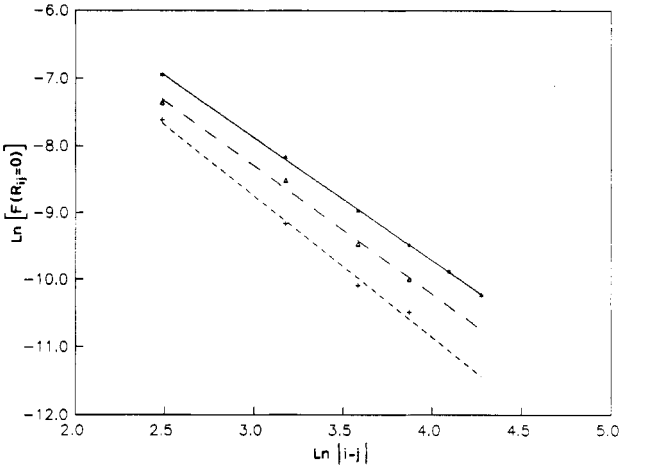

Figure 5. ln–ln plot of $F(R_{ij}=0)$ vs $|i\text{-}j|$ for a chain with N = 145 and cases A (*), B (△), and C (+).

second column of Table I (theoretical) and a common value for t, t = 2.43, consistent with eq 2 and the theoretical value of ν indicated above. Figure 2 shows the different results obtained for $F(R_{ij})$ in case C for an excluded-volume chain with N = 145. It can be observed that there is an increasing agreement with the des Cloizeaux universal curve, i.e., eq 4, as $|i\text{-}j|$ increases. Similar trends are found for the alternative cases A and B.

In Figure 3, we show results for $F(R_{ij})$ corresponding to cases A–C, obtained with $|i\text{-}j|$ = 72 (and N = 145 for cases B and C). The des Cloizeaux curves obtained for the three different cases, according to the renormalization group theory predictions for θ_0, θ_1, and θ_2, shown in the second column of Table I, are also plotted for comparison. The quantitative agreement of our results with these curves can be considered as satisfactory. Using values of θ_1 and θ_2 derived from the Baumgärtner simulations[8] (contained in the third column of Table I), one obtains curves for $F(R_{ij})$ which differ more significantly from our Monte Carlo data. Previous numerical data based on exact enumeration techniques in lattice models[6,14-16] (shown in the fourth column of Table I) are also in poorer agreement with the theory. (In the previous comparisons[6,8,14-16] of simulation data with eq 4, both exponents θ_k and t needed to be varied in order to obtain satisfactory fits to the scaling forms predicted for $F(R_{ij})$ at small and large values of R_{ij}.)

In Figure 4, we show our numerical results in a semilog plot which helps us to discern the short-range behavior. Results obtained with a higher value of N, N = 313, are included for the cases involving inner units, B and C. The scaling form predicted by the des Cloizeaux function (eq 4), in the small R_{ij} limit using the theoretical values of the exponents θ_k predicted by the renormalization group theory, is represented by straight lines; within statistical error, they are in good agreement with the simulation data. The disagreement with theory in a similar analysis of the Baumgärtner data[8] led to the alternative set of numerical exponents mentioned above. At large R_{ij}, the three cases merge in a universal curve, and the results involving inner units, corresponding to cases B and C, are shown to be also independent of N.

In Figure 5 we have plotted the results obtained for the cyclization probability $F(R_{ij}=0)$ vs $|i\text{-}j|$ for the same chain. Fits of these results to the equation

$$F(R_{ij}=0) \sim |i\text{-}j|^{-\alpha} \tag{9}$$

yield the values α_0 = 1.84 ± 0.02 for case A (cyclization through the end units), α_1 = 1.9 ± 0.2 for case B (cyclization through an end and an inner unit), and α_2 = 2.1 ± 0.1 for case C (cyclization from inner units), which are in fair agreement with the results calculated from the des

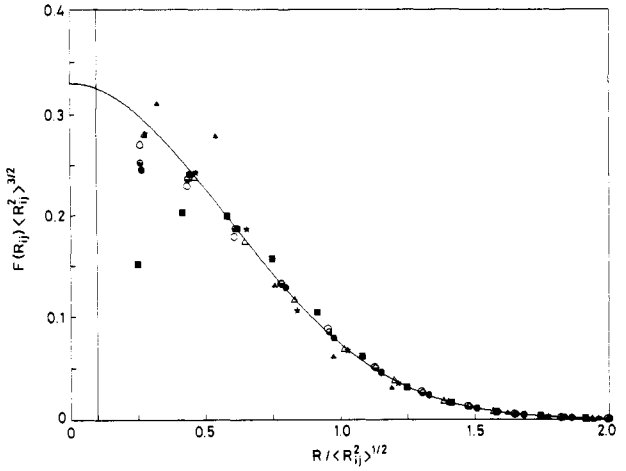

Figure 6. Results of $F(R_{ij})\langle R_{ij}^2\rangle^{3/2}$ vs $R_{ij}/\langle R_{ij}^2\rangle^{1/2}$ for a chain with $N = 73$, $|i-j| = 36$, and different values of ϵ/k_BT (close to the Θ conditions). Case A, $\epsilon/k_BT = 0.3$ (○) and 0.35 (△); case B, $\epsilon/k_BT = 0.3$ (◒); case C, $\epsilon/k_BT = 0.275$ (■), 0.3 (●), 0.325 (★), and 0.35 (▲). Solid line, eq 1. The vertical bar indicates the onset of the Lennard-Jones short-distance repulsive range.

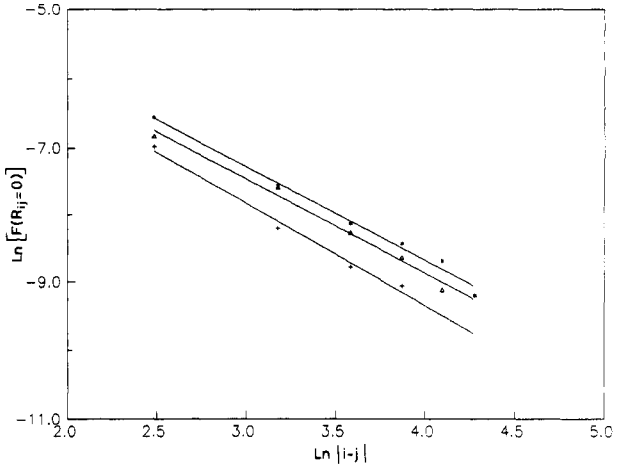

Figure 7. ln–ln plots of $F(R_{ij}=0)$ vs $|i-j|$ in Θ conditions for cases A (*), B (△), and C (+). Results for cases B and C are obtained from a chain with $N = 145$.

Cloizeaux function and eq 8 with $\nu \cong 3/5$: $\alpha_0 = 1.93$, $\alpha_1 = 2.04$, and $\alpha_2 = 2.18$. Previous simulations[15,16] have yielded values for α_1 in the range 2.10–2.18.

(b) Θ State. Previous data for different equilibrium properties have shown that quasi-ideal behavior (e.g., a quadratic mean radius of gyration proportional to N) is observed at values of ϵ/k_BT which are slightly dependent on the range of chain lengths.[9,10] Therefore, we have explored the distribution of distances in the Θ region by performing simulations with several different choices for this parameter. The Monte Carlo sampling cannot be as efficient for these less extended conformations and, therefore, we have had to restrict our calculations to shorter chains in order to obtain similar statistics. Fittings to the scaling law given by eq 8 yield values for the apparent exponent ν close to $1/2$ in the three cases A–C, which confirms the quasi-ideal behavior in the chosen range of the energy parameter.

In Figure 6 we show the $F(R_{ij})$ results obtained for case C (inner units) for $|i-j| = 36$ in a chain of 73 units, and different values of ϵ/k_BT corresponding to the Θ and sub-Θ (in terms of temperature) regions. It can be observed that the choice $\epsilon/k_BT = 0.3$ reproduces the Gaussian behavior for a wide range of values of R_{ij}, although there are significant deviations downward from the Gaussian curve for small values of the distance. The results for this value of ϵ/k_BT and cases A and B are also included in Figure 6. Although the three different cases tend to merge to the universal Gaussian behavior for longer values of R_{ij}, case A (involving only end units) yields a better description of the Gaussian behavior in the small R_{ij} region.

The differences between data corresponding to the three cases have a clear dependence on ϵ/k_BT. At the sub-Θ value of $\epsilon/k_BT = 0.35$ we find a remarkable agreement between the simulation data and the Gaussian curve at small R_{ij} for case A (these results are likewise included in Figure 6). Although the statistical accuracy is limited at small values of R, the results for case C are significantly different. The data suggest that the distribution of distances between inner units is clearly non-Gaussian, with a narrower form indicative of a more compact globular packing of the inner units. As the temperature is lowered, it appears that the process of collapse is initiated in the central part of the chain.

Figure 7 shows our results for the cyclization probabilities, $F(R_{ij}=0)$ vs $|i-j|$ in the Θ region, for cases A–C (the results involving inner units have been obtained for a chain with $N = 145$). The plotted linear fits yield exponents $\alpha_0 \simeq \alpha_1 = 1.4 \pm 0.1$ and $\alpha_2 = 1.5 \pm 0.1$, i.e., in agreement with the theoretical prediction of a common value, $3/2$, for an unperturbed (Gaussian) chain. Then, though the cyclization values are higher when external units are involved, their dependence on $|i-j|$ seems to reproduce a common quasi-ideal behavior.

Main Conclusions

(1) Our simulation data for $F(R_{ij})$ in the excluded-volume region in cases A (i and j end units), B (i end unit, j inner unit, or vice versa), and C (i and j inner units) are in good quantitative agreement with the des Cloizeaux predictions calculated with the exponents θ_k and t obtained from the renormalization group theory. The cyclization rate constants obtained numerically show $|i-j|$ dependencies also consistent with the theoretical predictions.

(2) The results for $F(R_{ij})$ for the Θ region all show agreement with a Gaussian curve in the three cases A–C with the same parameter of $\epsilon/k_BT = 0.3$ that was employed for the Θ state in previous studies.[9,10] However, the three cases show different features at small values of R_{ij}, and these differences are found to be dependent on ϵ/k_BT. A higher value of $\epsilon/k_BT = 0.35$ tends to improve the agreement with the Gaussian curve for case A, while the results for case C indicate non-Gaussian effects consistent with the onset of collapse. The cyclization rate constants exhibit a common quasi-ideal dependence on $|i-j|$ in the Θ region.

Acknowledgment. This research has been supported by Grant No. 0093/89 of the DGICYT (Spain), a British–Spanish joint research program (Project A111, 1991), the NATO Collaborative Research Grants Programme (Grant No. CRG 911005), and the donors of the Petroleum Research Fund, administered by the American Chemical Society.

References and Notes

(1) Yamakawa, H. *Modern Theory of Polymer Solutions*; Harper and Row: New York, 1971.
(2) de Gennes, P.-G. *Scaling Concepts in Polymer Physics*; Cornell University Press: Ithaca, NY, 1979.
(3) des Cloizeaux, J.; Jannink, G. *Polymers in Solution. Their Modelling and Structure*; Clarendon Press: Oxford, U.K., 1990.
(4) des Cloizeaux, J. *J. Phys.* **1980**, *41*, 223.
(5) Oono, Y.; Ohta, T. *Phys. Lett.* **1981**, *85A*, 480.

(6) Redner, S. *J. Phys. A* **1980**, *13*, 3525.
(7) Bishop, M.; Clarke, J. H. R.; Rey, A.; Freire, J. J. *J. Chem. Phys.* **1991**, *95*, 4589. Rey, A.; Freire, J. J.; García de la Torre, J. *Polymer* **1991**, *33*, 3477.
(8) Baumgärtner, A. *Z. Phys. B* **1981**, *42*, 265.
(9) Freire, J. J.; Pla, J.; Rey, A.; Prats, R. *Macromolecules* **1986**, *19*, 452.
(10) Freire, J. J.; Rey, A.; Bishop, M.; Clarke, J. H. R. *Macromolecules* **1991**, *24*, 6494.
(11) Webman, I.; Lebowitz, J. L.; Kalos, M. H. *Macromolecules* **1981**, *14*, 1495.
(12) Baumgärtner, A. *J. Chem. Phys.* **1982**, *76*, 4275.
(13) Semlyen, J. A. *Cyclic Polymers*; Elsevier: London, 1986.
(14) Martin, J. L.; Sykes, M. F.; Hioe, F. T. *J. Chem. Phys.* **1966**, *46*, 3478.
(15) Guttmann, A. J.; Sykes, M. F. *J. Phys.* **1973**, *C6*, 945.
(16) Whittington, S. G.; Trueman, R. E.; Wilker, J. B. *J. Phys.* **1975**, *A8*, 56.